International Journal for Parasitology 49 (2019) 311–320

Contents lists available at ScienceDirect

International Journal for Parasitology

journal homepage: www.elsevier.com/locate/ijpara

Somatic proteome of *Haemonchus contortus*

Tao Wang [a,1], Guangxu Ma [a,1], Ching-Seng Ang [b], Pasi K. Korhonen [a], Rong Xu [c], Shuai Nie [b], Anson V. Koehler [a], Richard J. Simpson [c], David W. Greening [c], Gavin E. Reid [d,e,f], Nicholas A. Williamson [b], Robin B. Gasser [a,*]

[a] Department of Veterinary Biosciences, Melbourne Veterinary School, The University of Melbourne, Parkville, Victoria 3010, Australia
[b] Bio21 Mass Spectrometry and Proteomics Facility, The University of Melbourne, Melbourne, Victoria 3010, Australia
[c] Department of Biochemistry, La Trobe Institute for Molecular Science (LIMS), La Trobe University, Bundoora, Victoria 3086, Australia
[d] School of Chemistry, The University of Melbourne, Parkville, Victoria 3010 Australia
[e] Department of Biochemistry and Molecular Biology, The University of Melbourne, Parkville, Victoria 3010, Australia
[f] Bio21 Molecular Science and Biotechnology Institute. The University of Melbourne, Parkville, Victoria 3010, Australia

ARTICLE INFO

Article history:
Received 21 October 2018
Received in revised form 12 December 2018
Accepted 17 December 2018
Available online 14 February 2019

Keywords:
Proteome
Parasitic nematode
Haemonchus contortus
Feeding
Metabolism
Development
Parasite-host cross-talk
Immunomodulation

ABSTRACT

Currently, there is a dearth of proteomic data to underpin fundamental investigations of parasites and parasitism at the molecular level. Here, using a high throughput LC–MS/MS-based approach, we undertook the first reported comprehensive, large-scale proteomic investigation of the barber's pole worm (*Haemonchus contortus*) – one of the most important parasitic nematodes of livestock animals worldwide. In total, 2487 unique *H. contortus* proteins representing different developmental stages/sexes (i.e. eggs, L3s and L4s, female (Af) and male (Am) adults) were identified and quantified with high confidence. Bioinformatic analyses of this proteome revealed substantial alterations in protein profiles during the life cycle, particularly in the transition from the free-living to the parasitic phase, and key groups of proteins involved specifically in feeding, digestion, metabolism, development, parasite-host interactions (including immunomodulation), structural remodelling of the body wall and adaptive processes during parasitism. This proteomic data set will facilitate future molecular, biochemical and physiological investigations of *H. contortus* and related nematodes, and the discovery of novel intervention targets against haemonchosis.

1. Introduction

Parasitic worms cause substantial mortality and morbidity in animals, and major losses to food production worldwide. Roundworms (=nematodes) cause destructive diseases that affect hundreds of millions of livestock animals (e.g., sheep, goats and cattle), resulting in economic losses of tens of billions of dollars per annum globally (Roeber et al., 2013; Gasser and von Samson-Himmelstjerna, 2016). Despite substantial efforts to control these worms, commercial vaccines are lacking and treatment relies heavily on only a relatively small number of drugs (anthelmintics). As drug resistance is now widespread, there is an urgent need to develop new and effective interventions, built on a solid understanding of these worms, their relationship with animal host(s) and parasitism at the molecular level.

Advanced nucleic acid sequencing and bioinformatic technologies have enabled an unprecedented number of worm genomes to be decoded (e.g., Laing et al., 2013; Schwarz et al., 2013, 2015; Tang et al., 2014; Tyagi et al., 2015; Korhonen et al., 2016). Although draft genomes provide investigators with resources to explore these worms at the molecular level, the expression profiles and functions of most parasite proteins are unknown. Researchers have begun using genomic sequence data sets to assist investigations of the expression, localisation and function of genes employing advanced transcriptomic and proteomics tools.

While transcriptomics can quantify RNAs, such as messenger and small RNAs, advanced proteomics provides a means of identifying and quantifying proteins in whole worms, dissected tissues or particular developmental stages (Bennuru et al., 2011; Morris et al., 2015). The digital resources ('tool-kits') to investigate and mine genomic and transcriptomic data sets are now available. The databases NEMBASE (Parkinson et al., 2004) and Nematode.net (Martin et al., 2015) contain relatively extensive genomic and/or transcriptomic datasets, and ParaSite (Howe et al., 2016) provides a wealth of information and features in WormBase for key parasitic

* Corresponding author.
E-mail address: robinbg@unimelb.edu.au (R.B. Gasser).
[1] Joint first authors.

https://doi.org/10.1016/j.ijpara.2018.12.003
0020-7519/

worms. However, a critical appraisal of current literature reveals that, with the exception of selected filarioid nematodes (Bennuru et al., 2011; Armstrong et al., 2016), comprehensive proteomic data sets are scant for most other socio-economically important parasitic nematodes, despite the massive technological advances made in recent years in the field of proteomics (Zhang et al., 2013; Aebersold and Mann, 2016).

The aim of the present study was to define the proteome of one of the most important parasitic nematodes of livestock animals worldwide, *Haemonchus contortus*, using high throughput liquid chromatography–mass spectrometry (LC–MS/MS), and explore biological pathways enriched during parasitism, employing advanced informatics and current genomic/transcriptomic resources (cf. Schwarz et al., 2013; Preston et al., 2017; Ma et al., 2018).

Haemonchus belongs to one of the largest orders of nematodes (Strongylida) which adversely impact on the health and wellbeing of animals (Gasser and von Samson-Himmelstjerna, 2016). It is a blood-feeding (haematophagous) worm of the stomach (abomasum) of ruminants, causing a disease, called haemonchosis, leading to anaemia and/or associated complications, ill thrift and death in severely affected animals (Gasser and von Samson-Himmelstjerna, 2016). This worm is transmitted orally from contaminated pasture to the host through a direct life cycle: eggs are excreted in host faeces; individual L1s develop inside eggs to then hatch (within 1 day) and develop through to L2s and L3s) in about a week; the infective L3s are then ingested by the host, exsheath (xL3s) and develop via the L4 stage to dioecious haematophagous adults (within 3 weeks) in the stomach (Veglia, 1915). Given the scant proteomic data available for parasitic nematodes (i.e. cuticular proteins, excretory/secretory (ES) proteins and extracellular vesicles) (Yatsuda et al., 2003; Hewitson et al., 2008; Wang et al., 2013; Buck et al., 2014; Chehayeb et al., 2014; Liu et al., 2015; Zamanian et al., 2015; Tzelos et al., 2016; Sperotto et al., 2017; Stoltzfus et al., 2017), defining the first proteome representing key developmental stages of *H. contortus* will facilitate elucidating aspects of its unique biology and its ability to survive and maintain a complex relationship with its host animal, which could open the door to discovering new interventions against this and related worms.

2. Materials and methods

2.1. Parasite stages

Haemonchus contortus was produced in Merino lambs (3 months of age; Victoria, Australia), maintained under helminth-free conditions (animal ethics approval no. 1714374, The University of Melbourne, Australia). Different developmental stages/sexes of *H. contortus*– i.e. eggs. L3s and L4s, female (Af) and male (Am) adults – were produced as described previously (Campbell et al., 2008; Schwarz et al., 2013). Briefly, sheep were inoculated intraruminally (via oral intubation) with 7000 infective L3s of *H. contortus*. Eggs were isolated from the faeces from infected sheep (1 month after inoculation) using a sucrose flotation procedure (Mes et al., 2007). L3s were produced in culture as described previously (Nikolaou et al., 2002). L4s and adults (Af and Am) were collected from the abomasa of infected sheep 9 and 28 days after the inoculation of sheep with L3s, respectively. Four biological replicates of each developmental stage were prepared, washed extensively (five times) in 50 ml volumes of physiological saline (pH 7.0), pelleted and then frozen at −80 °C until further analysis.

2.2. Protein extraction

Proteins were extracted from each of four replicates of each egg, L3, L4, Af and Am. In brief, ~30,000 eggs or larvae, or 100 adults, were transferred to sterile (1.5 mL) Eppendorf tubes containing 500 µL of lysis buffer (8 M urea in 100 mM triethyl ammonium bicarbonate, pH 8.5). Each sample was then subjected to three freeze (−196 °C) – thaw (37 °C) cycles (Caito and Aschner, 2015) and centrifuged at 10,000*g* for 30 s, ultra-sonicated (20 kHz) using a BioRuptor (10 cycles: 30 s on−30 s off) on ice. Each sample was supplemented with protease inhibitor cocktail set I (Merck, Denmark) and incubated at 23 °C for 30 min. Then, samples were centrifuged at 12,000*g* for 30 min, and the supernatants collected for analyses. Protein concentrations were measured using a BCA Protein Assay Kit (Thermo Fisher Scientific, USA).

2.3. In-gel and in-solution digestion, and LC–MS/MS analysis

The analysis of the proteome of *H. contortus* was conducted using in-gel and in-solution digestion protocols, as described previously (Ang et al., 2011). For the in-gel procedure, samples containing proteins from the egg, L3, L4, Af *and* Am stage (30 µg of each) were resolved in a pre-cast NuPAGE 4–12% Bis-Tris gel (Invitrogen, USA) at 150 V (constant) for 1 h. The gel was stained with Coomassie blue for 10 h (shaking) and destained with H_2O. The gel lane was sliced into 10 equal pieces, reduced with 10 mM tris (2-carboxyethyl) phosphine (TCEP) at 55 °C for 45 min, then alkylated with 55 mM iodoacetamide in the dark at 22 °C for 30 min, followed by a digestion with sequencing-grade, modified trypsin (Pierce, USA) at 37 °C for 16 h. Samples were spiked with Hyper Reaction Monitoring (HRM) calibration peptides (Biognosys, Switzerland) prior to LC–MS/MS analysis.

For the in-solution procedure, samples containing proteins (100 µg) from either the egg, L3, L4, Af *or* Am stage were reduced with 10 mM TCEP at 55 °C for 45 min, then alkylated with 55 mM iodoacetamide in the dark at 22 °C for 30 min, followed by a double-digestion with Lys-C/trypsin mix (Promega, USA) at 37 °C for 16 h (4 h for Lys-C digestion and 12 h for trypsin digestion). The tryptic samples were acidified with 1.0% (v/v) formic acid, purified using Oasis HLB cartridges (Waters, USA). Proteins in these samples were divided into eight fractions using the high pH reversed-phase peptide fractionation kit (Pierce, USA) according to the manufacturer's protocol. All fractions were freeze-dried prior to re-suspension in aqueous 2% w/v acetonitrile and 0.05% trifluoroacetic acid (TFA) w/v, and were spiked with HRM calibration peptides (Biognosys, Switzerland) before LC–MS/MS analysis.

2.4. Data-dependent LC–MS/MS

For data-dependent acquisition (DDA) profiling, tryptic peptides were analysed using the Q Exactive Plus Orbitrap and Fusion Lumos Orbitrap mass spectrometers (Thermo Fisher, USA), in order to achieve the highest possible proteome coverage in relation to the *H. contortus* genome. The LC system was equipped with an Acclaim Pepmap nano-trap column (Dinoex-C18, 100 Å, 75 µm × 2 cm) and an Acclaim Pepmap RSLC analytical column (Dinoex-C18, 100 Å, 75 µm × 50 cm). The tryptic peptides were injected into the enrichment column at an isocratic flow of 5 µL/min of 2% v/v CH_3CN containing 0.1% v/v formic acid for 6 min, applied before the enrichment column was switched in-line with the analytical column. The eluents were 0.1% v/v formic acid (solvent A) and 100% v/v CH_3CN in 0.1% v/v formic acid (solvent B). The gradient was at 300 nl/min from (i) 0–6 min at 3% B; (ii) 6–95 min, 3–20% B; (iii) 95–105 min, 20–40% B; (iv) 105–110 min, 40–80% B; (v) 110–115 min, 80–80% B; (vi) 115–117 min 85–3% and equilibrated at 3% B for 10 min before injecting the next sample. The Q Exactive Plus mass spectrometer was operated in the data-dependent mode, whereby full MS1 spectra were acquired in a positive mode, 70,000 resolution, AGC target of $3e^6$ and maximum

IT time of 50 ms. Fifteen of the most intense peptide ions with charge states of ≥2 and intensity thresholds of ≥$1.7e^4$ were isolated for MSMS. The isolation window was set at 1.2 m/z, and precursors fragmented using a normalised collision energy of 30, a resolution of 17,500, an AGC target of $1e^5$ and a maximum IT time of 100 ms. Dynamic exclusion was set at 30 s. The Fusion Lumos mass spectrometer was operated in positive-ionisation mode, with the spray voltage set at 1.9 kV and the source temperature at 275 °C. The mass spectrometer was operated in the data-dependent acquisition mode, whereby full MS1 spectra were acquired in a positive mode at 120,000 resolution, with an AGC target of $5e^5$. The "top speed" acquisition method mode (cycle time: 3 s) on the most intense precursor was used, whereby peptide ions with charge states of 2–5 were isolated using an isolation window of 1.2 m/z and fragmented with a high energy collision (HCD) mode employing a stepped collision energy of 30 ± 5%. Fragment ion spectra were acquired in Orbitrap at 15,000 resolution. Dynamic exclusion was activated for 30 s.

2.5. Data-independent LC–MS/MS

Data-independent acquisition (DIA) was carried out on the Q Exactive Plus mass spectrometer using the HRM-DIA methodology (Bruderer et al., 2015). Here, a survey scan from 400 to 1000 m/z at 70,000 resolution and an AGC target of $3e^6$ at 50 ms was followed by 30, 21 m/z DIA windows at 17,500 resolution, AGC of $1e^6$ and the IT time set at "auto". Stepped normalised collision energies were set at 28, 30 and 32. All spectra were acquired in the profile mode.

2.6. Protein identification and quantification

Protein/peptide identification and subsequent spectral library generation were conducted using Proteome Discoverer (v.2.1, Thermo Fischer Scientific) with the Sequest HT search engine and the Percolator semi-supervised learning algorithm (Kall et al., 2007). An in-house sequence database, with GenBank's non-redundant protein database (NR) annotation, was established for *H. contortus* (16,093 protein entries) based on transcriptomes (Schwarz et al., 2013; Preston et al., 2017; Ma et al., 2018), PacBio (long sequence) reads (Bioproject: PRJEB2252 at NCBI) and additional, curated protein data for *H. contortus* (494 protein entries) (Mohandas et al., 2015, 2016; Stroehlein et al., 2015), and the Biognosys iRT peptides. Search parameters were: a precursor tolerance of 20 ppm, MSMS tolerance of 0.05 Da, fixed modifications of carbamidomethylation of cysteine (+57 Da) and methionine oxidation (+16 Da). Peptides were accepted based on a false discovery rate (FDR) of <0.01 at both the peptide and protein levels. For stage-specific identification and relative quantification comparisons, only protein identifications with ≥2 peptides and present in ≥3 biological replicates of at least one developmental stage were accepted.

HRM-DIA-based quantitation was carried out using Spectronaut software (Biognosys, v.11). The spectral library used for the database search contained 3746 protein groups (34,282 peptides), generated from a total of 65 in-gel-digested and basic reverse phase-separated peptide DDA experiments from the Q Exactive Plus mass spectrometer workflow. To achieve optimal quantitation, we used instrument-specific libraries, and employed the same chromatographic conditions. Results were exported and analysed in Spectronaut using default settings and a stringent q-value cut-off (<0.01). For each protein, three peptides with the highest intensities were used for quantitative analysis. The data were normalised based on the median protein intensity under each condition. Fold-change thresholds of ≥2, with the inferior q-value set at ≤0.05, were used to establish whether a protein was up- or down-regulated. The P values were adjusted using a Benjamini-Hochberg correction. Results are available via the PRIDE data repository (accession number: PXD009956).

2.7. Bioinformatic analyses of data sets

The UniProt repository was used for protein annotation (cellular compartment, subcellular location, transmembrane region or molecular function). Molecular functions of proteins predicted from the genome of *H. contortus*, or identified or quantified in the proteome of *H. contortus*, were classified according to Gene Ontology (GO) using the program InterProScan (Mitchell et al., 2015). Multi-scatter plots were drawn using Perseus software (v.1.6.1.1) using default settings (Tyanova et al., 2016). Principal component analysis (PCA) and hierarchical cluster analysis (HCA) were conducted in the R language using software packages Glimma v.1.2.1 and gplots v.3.0.1. The statistical significance of correlation analyses was set at $P < 0.05$. Biological functions were assigned to differentially expressed proteins using the Kyoto Encyclopedia of Genes and Genomes (KEGG) databases (Kanehisa et al., 2016). KEGG pathway annotation was conducted employing KEGG BLAST hits (*E*-value: $<10^{-5}$) and corresponding KEGG Orthology (KO) terms (Mao et al., 2005). KO terms were then assigned to KEGG pathways and KEGG BRITE orthologous protein families by mapping these terms to the KEGG Orthology Based Annotation System (KOBAS) database (Xie et al., 2011). Enriched KEGG pathways were identified using a cut-off of $P < 0.01$ (Fisher's Exact test). KEGG functional enrichments of differentially expressed proteins were integrated and displayed using the program FuncTree (Uchiyama et al., 2015). Particular sequences, such as those of collagens and cuticular proteins, were compared with those available in WormBase (Howe et al., 2016) using blastp. Protein expression linked to lipid metabolism, expressed as total ion abundance of lipids ($n = 554$), was calculated in different stages/sexes of *H. contortus* from a recently published, label-free relative quantitation lipidome analysis data set (Wang et al., 2018). A one-way ANOVA test was performed for multiple group comparisons using GraphPad Prism 6.0 software (GraphPad, La Jolla, USA). Statistical significance was set at $P < 0.05$.

3. Results

3.1. The somatic proteome of H. contortus

The proteome of *H. contortus* (Haecon 5 strain) was inferred from in-gel digested and basic reverse phase-separated peptides from key developmental (i.e. egg, L3, L4 and adult) stages of *H. contortus*. Amongst 62,080 peptides (with lengths of between six and 47 amino acids), we identified 4071 protein groups (Supplementary Table S1). Of 1946 (47.8%) orphan proteins (with unknown identity and function) identified, 99.8% ($n = 1942$) had relatively conserved homologs in various secernentean nematodes (such as *Ancylostoma ceylanicum*, *Angiostrongylus cantonensis*, *Ascaris suum*, *Brugia malayi*, *Caenorhabditis* spp. and *Loa loa*). This represents 24.5% of the proteins predicted from the in-house sequence database of *H. contortus* (see Section 2; cf. Schwarz et al., 2013; Mohandas et al., 2015, 2016; Stroehlein et al., 2015; Preston et al., 2017; Ma et al., 2018).

3.2. Quantification of proteins in different developmental stages of H. contortus

From the somatic proteome, we used peptides identified only from the Q Exactive Plus mass spectrometer in order to construct an instrument-specific spectral library for quantitative analysis employing the HRM-DIA method (Bruderer et al., 2016). This

library consists of 3746 unique proteins and 34,282 peptides. A total of 2487 unique proteins representing all key developmental stages/sexes (i.e., egg, L3, L4, Af and Am) of *H. contortus* were identified and quantified with high confidence in the spectral library based on stringent criteria. The greatest number of proteins identified was in the egg stage (n = 1744), followed by L4 (n = 1697), Af (n = 1677) and Am (n = 1604), followed by L3 (n = 1208). The full list of proteins identified in each developmental stage is given in Supplementary Table S2. The comparisons of the identified proteins amongst different developmental stages of *H. contortus* are shown in a Venn diagram (Fig. 1A). Overall, most proteins (n = 1915, 77.0%) were shared by at least two developmental stages of *H. contortus*. Of these shared proteins, 753 (30.3%) were detected in all developmental stages studied.

To gain insights into parasitic stages (i.e. L4, Af and Am), 415 stage-specific proteins were identified. Conspicuous among them were molecules such as collagens and cuticular proteins (n = 10), nematode SCP/TAPS proteins (n = 19) and cysteine peptidases (n = 15). Within a particular developmental stage, the relative ratios of proteins expressed in individual stages ranged from 1.4% to 21.6%. Notably, the largest stage-specific set of proteins identified was in the egg (n = 376, 21.6%), followed by the free-living L3 stage (n = 106, 8.8%), whereas smaller numbers of proteins were enriched in the parasitic stages (L4 (n = 43, 2.5%), Af (n = 25, 1.5%) and Am (n = 22, 1.4%)).

The distribution of the molecular functions (GO level 2) of proteins identified in each stage, according to GO, is summarised in Fig. 1B. Most proteins were associated with binding (GO: 0005488; 45.1–50.5%) and catalytic activity (GO: 0003824; 36.4–40.5%) in individual stages. Each of these two major functional cat-

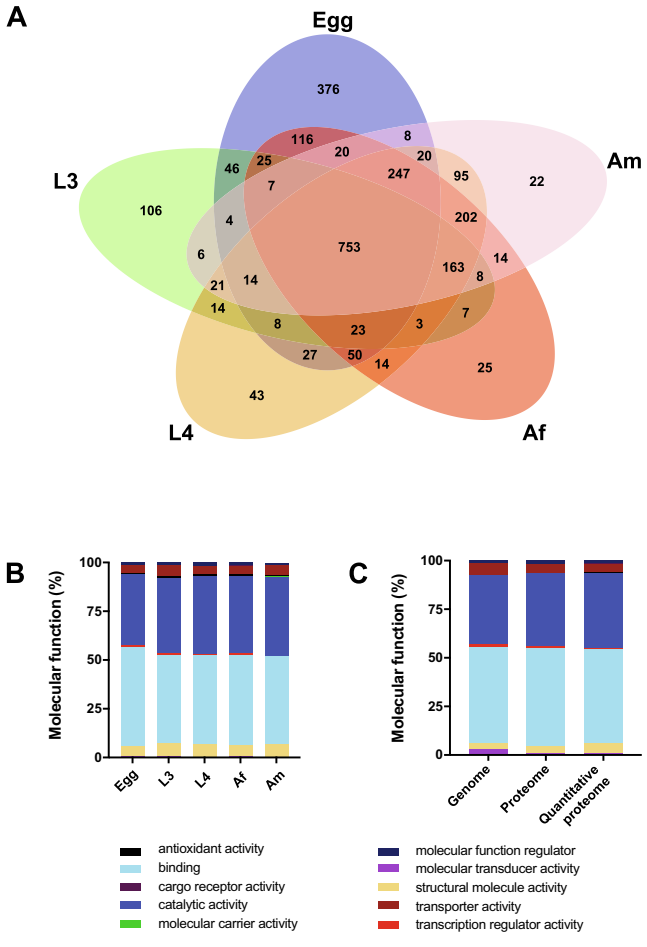

Fig. 1. *Haemonchus contortus* proteins and molecular functions. (A) Venn diagrams showing the numbers of quantified proteins unique to or shared by different developmental stages of *H. contortus* (egg, L3, L4, female (Af) and male (Am) adults). (B) The distribution of the molecular functions (Gene Ontology (GO) level 2) of proteins quantified in each stage. Distribution was expressed as a percentage of the total number of proteins identified in a particular stage, to allow quantitative comparisons among different developmental stages of *H. contortus*. (C) The distribution of the molecular functions (GO level 2) of predicted or identified proteins. Distribution was expressed as a percentage of the total number of proteins, to allow quantitative comparisons on the genome, qualitative and quantitative proteome levels.

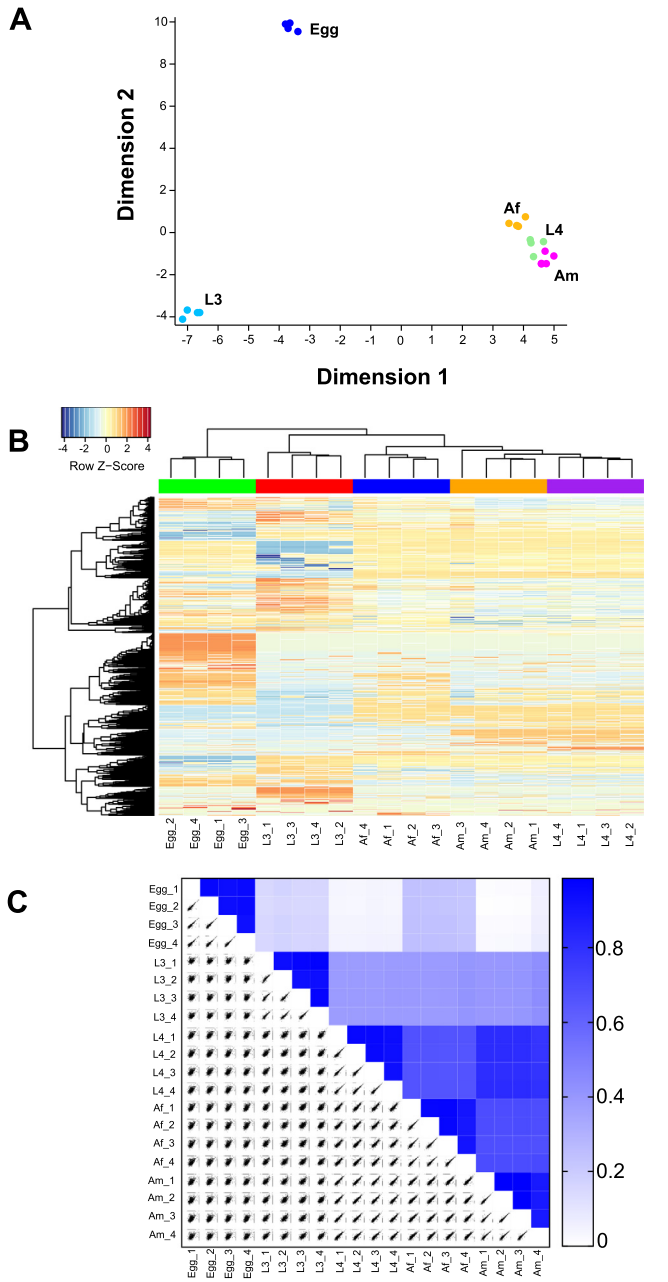

Fig. 2. Analyses of the somatic proteome of *Haemonchus contortus*. (A) Principal component analysis (PCA) of the somatic proteome representing eggs, L3s, L4s, female (Af) and male (Am) adults of *H. contortus*. (B) Hierarchical cluster analysis (HCA) displaying the expression profiles for these distinct developmental stages/sexes. Normalised protein abundance is shown as a blue to red scale, depicting low to high protein abundance. (C) Multi-scatter plots showing the correlation between biological replicates of proteomic changes in developmental stages upon pairwise comparison. Dark blue represents a high Pearson's correlation between samples. Each stage was represented by biological quadruplicates.

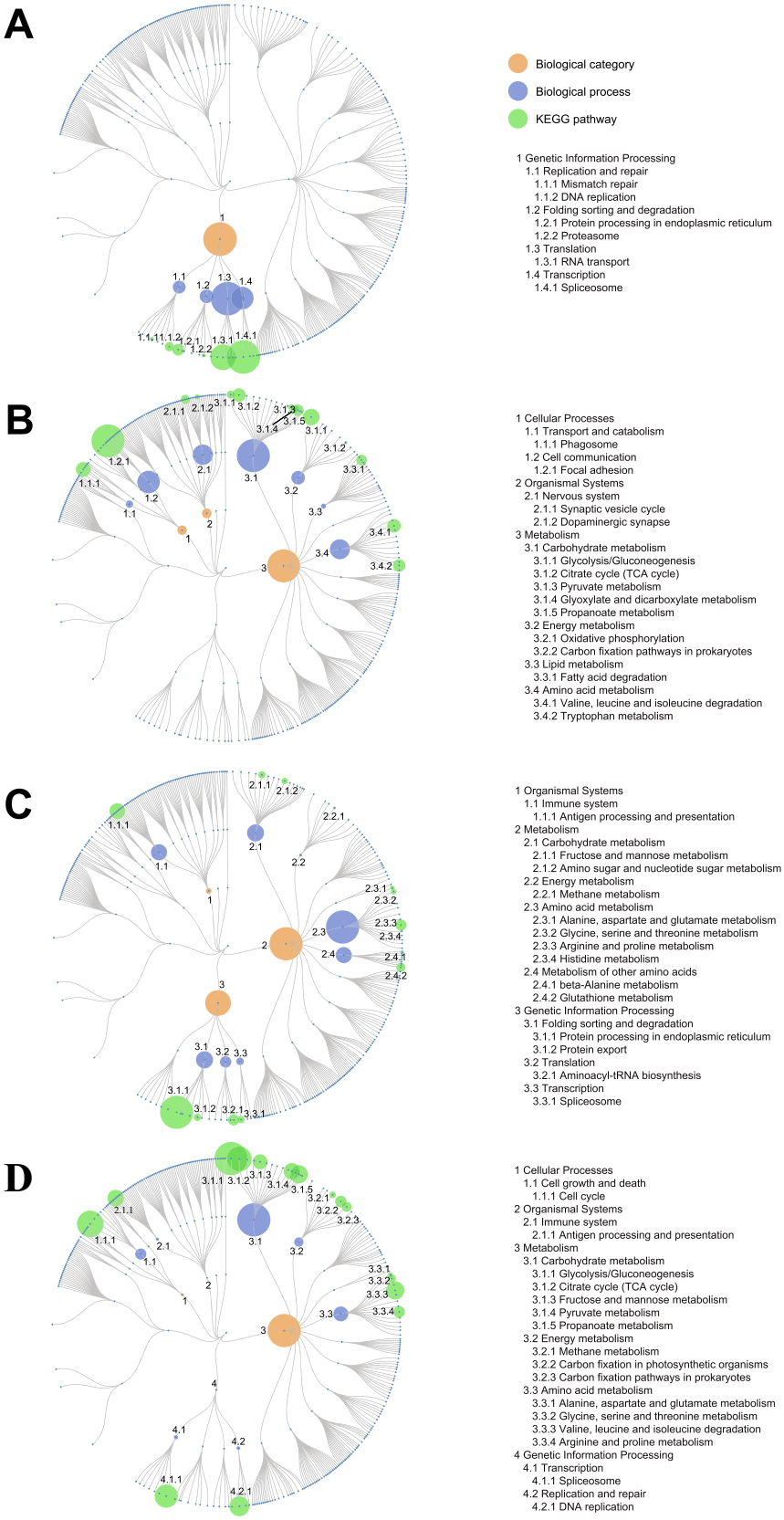

Fig. 3. Enriched biological processes and associated pathways (Kyoto Encyclopedia of Genes and Genomes, KEGG) of differentially expressed proteins in (A) egg, (B) L3, (C) L4, (D) adult female (Af) stages of *H. contortus*. Enriched annotations of highly expressed proteins (fold change (FC) of >2; false discovery rate (FDR) of <0.05) are listed. Dot sizes indicate counts of significantly highly expressed proteins (see also Supplementary Table S5).

egories (binding and catalytic activity) contained at least 490 annotated proteins, whereas proteins involved in structure, transporter and antioxidant activities were less represented. A closer appraisal of molecular functions (GO level 3) revealed proteins involved predominantly in the binding of compounds, ions, other proteins and small molecules, while hydrolase molecules were represented mainly by the 'catalytic activity' category (Supplementary Table S3). In terms of the percentages of proteins classified in each sub-category, there was no obvious difference among the developmental stages studied (Fig. 1B).

3.3. Comparison of molecular functions

A comparison of the molecular functions inferred for (i) proteins predicted from the genome, (ii) proteins identified in the proteome and (iii) proteins quantified in the proteome revealed a relative concordance in the proportions (percentages) of proteins present in particular functional groups (Fig. 1C, Supplementary Table S4). For all three datasets/analyses (i–iii), there was concordance in the percentages of predicted or identified proteins associated predominantly with activities of molecular carriers (0.01–0.04%), cargo receptors (0.04–0.05%), antioxidants (0.3–0.6%), transcription regulators (0.8–1.8%), molecular function (1.5–1.9%), structural molecules (3.2–5.3%) and transporter (4.2–5.8%), with binding (48.4–50.3%) and catalytic (35.4–38.3%) activities dominating. The only discrepancy seen related to 'molecular transducer activity' which was underrepresented in proteins identified (0.7%) and quantified (0.6%) in the proteome compared with those predicted from the genome (2.9%), indicating limited or no expression of some genes in the *H. contortus* genome, or expression levels that were not detectable using the present proteomic approaches.

3.4. Alterations in protein expression during development

PCA of the proteome of the distinct developmental stages/sexes of *H. contortus* was performed (Fig. 2A). The two-dimensional PCA showed that parasitic stages (i.e. L4, Af and Am) clustered tightly together, to the exclusion of the free-living stages (i.e. egg and L3). Interestingly, the difference between the two free-living stages was substantial. Following PCA, a hierarchical clustering showed a clear division of the proteomic data set into five distinct groups, corresponding to the different developmental stages of *H. contortus* (Fig. 2B). Moreover, together with multi-scatter plots (Fig. 2C), hierarchical clustering showed that the difference in expression within a particular stage (i.e. among the four replicates) was markedly less than differences among stages, allowing further comparisons of relative protein expression alterations during *H. contortus* development.

KEGG pathway enrichment analysis revealed that proteins expressed differentially between or among at least two developmental stages were involved in one to five biological categories (i.e. cellular processes, environmental information processing, genetic information processing, organismal systems and metabolism), covering key aspects of parasite growth and metabolism (Supplementary Table S5). In the egg stage, differentially expressed proteins were mainly linked to genetic information processing (n = 478 of 504), whereas only a limited number of differentially expressed proteins associated with metabolism (n = 14) and/or cellular processes (n = 12) (Fig. 3A). In the genetic information processing category, translation (n = 182; ribosome, RNA transport, aminoacyl-tRNA biosynthesis and mRNA surveillance pathway) and transcription (n = 126; spliceosome) were the two major processes in the egg stage, whereas 77 proteins were inferred to relate to replication and repair processes (i.e. DNA replication, mismatch repair, nucleotide excision repair and base excision repair). Two additional, enriched pathways (environmental information processing (n = 52) and organismal systems (n = 130)) were represented in the L3 stage, to the exclusion of eggs (Fig. 3B, Supplementary Table S5). Unlike the egg stage, only a limited number (n = 26) of differentially expressed proteins was involved in the genetic information processing pathway in the L3 stage. Notably, more than 350 of 715 proteins expressed in L3s were enriched in metabolic pathways including carbohydrate metabolism (n = 111; citrate cycle, glycolysis/gluconeogenesis, propanoate metabolism, glyoxylate and dicarboxylate metabolism, pyruvate metabolism and butanoate metabolism) as well as amino acid (n = 70), energy (n = 50) and lipid (n = 23) metabolism. Similar to the L3 stage, most differentially expressed proteins (n = 101 of 203) in the L4 stage were enriched within the metabolism category (Fig. 3C). This category was represented predominantly by amino acid (n = 58) and carbohydrate (n = 21) metabolism. The remaining categories of proteins specific to the L4 stage were inferred to be associated with genetic information processing (n = 79), organismal systems (n = 20) and environmental information processing (n = 3). For the adult stages, in addition to metabolism (n = 299), which was also a major biological category, genetic information processing (n = 34) and organismal systems (n = 14) were two categories represented by proteins enriched in Af (Fig. 3D), but this was not the case for Am. Only four differentially expressed proteins were detected in Am, all of which were inferred to be involved in carbohydrate metabolism (Supplementary Table S5).

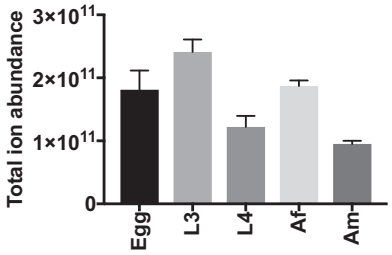

Fig. 4. Comparison of total ion abundance of lipids among different developmental stages/sexes of *Haemonchus contortus* (egg, L3, L4, female (Af) and male adults (Am)). Statistical analysis was performed by ANOVA ($^{**}P < 0.01$). Error bars indicate ± S.D. of the mean.

3.5. Lipid ion abundance

In total, 554 unique lipid species which represented four lipid categories (i.e. glycerolipids, glycerophospholipids, sphingolipids and sterol lipids) extracted from equal amounts (3 mg per stage) of freeze-dried nematode material were used to calculate the total ion abundance of lipids in different developmental stages/sexes of *H. contortus* (see Fig. 4, Supplementary Table S6). Abundance was highest in the free-living L3 stage, followed by Af (which contain eggs) and eggs (similar abundance), followed by L4 and Am (with lowest abundance compared with L3; $P < 0.01$). Notably, total ion abundance was markedly higher in Af than in Am and the L4 stage.

4. Discussion

By defining a comprehensive proteome from body tissues of key developmental stages (egg, L3, L4 and adult) and both sexes (adult) of *H. contortus*, we have been able to provide the first insights, at the protein level, into key biological processes and pathways enriched in stages of this pathogen that likely underpin parasitism in the host animal. In the developmental cycle of *H. contortus* and related strongylid nematodes, the infective (L3) stage is ingested, and the parasitic stages establish in the stomach (abomasum) of the ruminant, feed on blood and other tissues, and rapidly grow,

develop and reproduce within a period of 3 weeks. During this transition, one expects strictly controlled patterns of expression of particular protein groups relating to feeding, the acquisition of essential nutrients, metabolism as well as body structure and integrity, to meet major demands for worm growth and development within the host animal, and molecular processes (including host cross-talk and immune modulation) that ensure the survival of the parasite in a harsh, gastric environment (parasitism). These patterns are clearly reflected in the pathways enriched in the somatic proteome of *H. contortus*.

Although the results of the proteomic analysis of the free-living stages of *H. contortus* were relatively inconspicuous (Supplementary Table S2), this was not the case for the parasitic stages. The findings suggest that the L4s and adults (parasitic) rely heavily on the catabolism of haemoglobin for survival once established in a host, similar to other haematophagous parasites (Tort et al., 1999; Williamson et al., 2003). Peptidases, including aspartic peptidases, cysteine peptidases and metallopeptidases, are recognised as crucial molecules in the degradation of blood components, tissues and in anticoagulation, and are likely to be essential for growth, development and survival of *H. contortus* (see Williamson et al., 2003). Peptidases C1A (cysteine peptidases; $n = 15$), A1 (aspartic peptidases; $n = 9$), M12 (metallopeptidases; $n = 3$) and M13 (metallopeptidases; $n = 2$) were particularly abundant in the parasitic stages (Supplementary Table S2), in accord with transcriptomic data (Schwarz et al., 2013).

Pathway enrichment analysis highlighted the distinct metabolism (i.e. the proportion of enriched proteins dramatically increased from 3% in egg to more than 50% from the L3 stage onwards), reflecting the increasing demand for essential energy for their rapid growth during the transition from the free-living to parasitic phase of the parasite's life cycle. Enriched pathways included carbohydrate, amino acid, energy and lipid/fatty acid metabolism (cf. Fig. 3). These findings are in accord with previous results for the developmental transcriptome of *H. contortus* (see Schwarz et al., 2013), and suggest that metabolism is under tight post-transcriptional control in this haematophagous nematode. Unlike the relatively well controlled lipid metabolism in the developmental stages of *Caenorhabditis elegans* (see Cooper and Van Gundy, 1971; Ashrafi, 2007), lipid metabolism is down-regulated in *H. contortus* once this nematode reaches the parasitic stage. Here, we identified 23 relatively abundantly expressed proteins involved in the fatty acid degradation pathway in the L3 stage, whereas no enrichment in lipid-related metabolism was detected in parasitic stages (i.e. L4, Af and Am). This finding is consistent with the alterations observed in total lipid ion abundances in different stages of *H. contortus* (see Fig. 4, Supplementary Table S6), in which we recently indicated that *H. contortus* alters its lipidome to adapt to an 'opportunistic' way of life in the host animal (Wang et al., 2018). We hypothesise that *Haemonchus* tends to down-regulate its lipid metabolism (mainly energy storage lipids – triradylglycerols) to rely on a supply of corresponding fatty acids from blood and tissues once established at its predilection site (abomasum) in the host animal (Harder, 2016; Wang et al., 2018). Whether similar processes are active in other haematophagous nematodes is presently unknown and warrants future investigation.

Haemonchus contortus develops from infective L3s to reproductively active adults within 3 weeks. This parasitic phase is associated with rapid growth and development; a panel of at least 8, 14, 8 and 12 collagens and cuticular proteins are represented in the proteome of the L3, L4, Af and Am stages, respectively, whereas five are in the egg stage. Although there are differences in the numbers of predicted collagens between free-living stages ($n = 7$) and parasitic stages ($n = 4$–7), seven of them are common to L4, Af and Am (Supplementary Table S7). Such proteins are expected to be critical for the maintenance of body form, integrity, and for contact with the host interface and environment. An analysis of relative abundance indicated that these collagens and cuticular proteins are expressed mainly in the L4 and adult stages (Supplementary Table S7), coinciding with a peak of expression of prolyl 4-hydroxylase (Supplementary Table S2), a key enzyme involved in collagen synthesis and assembly. All 22 collagens and cuticular proteins identified have significant sequence similarity (23–73%) to 19 different collagens of *C. elegans* (Supplementary Table S7). The collagens of *H. contortus* are not closely related to those shown to be crucial for cuticle synthesis in *C. elegans* (i.e. are not DPY-2, -3, -7, -8, -10 and -13) (Page and Johnstone, 2007), indicating significant differences in cuticle synthesis between this free-living nematode and *H. contortus*. The marked growth of *H. contortus* following its moults may be explained by cuticle extension and expansion, and previous work on *H. contortus* has shown that there is a marked increase in the thickness of both the basal and median layers of the cuticle when the L4 (0.089–0.13 μm) develops to the adult stage (0.28–0.41 μm) (Veglia, 1917). Thus, it is likely that the relatively high numbers of collagens and cuticular proteins relate to rapid growth and developmental transitions in *H. contortus* throughout its life cycle.

Parasitic worm proteins that belong to the cysteine-rich secretory proteins, antigen 5 and pathogenesis-related 1 (CAP) superfamily (Gibbs et al., 2008) are recognised to play key roles in the infection process, in growth and development and/or modulation of immune responses in host animals (Hewitson et al., 2015). Here, we detected 21 SCP/TAPS family proteins, 19 of which were detected in the L4 and adult stages, but not the free-living stages of *H. contortus* (see Supplementary Table S8). We propose that that the 19 SCP/TAPS proteins in the parasitic stages play central roles in development, reproductive processes and/or the parasite-host interplay, and that the two others (i.e. HCON_10053s and HCON_11608s) have roles in the development of eggs or free-living larval stages. These hypotheses need to be tested in extensive experimental investigations.

A previous genomic study predicted genes encoding 84 SCP/TAPS proteins (22 double and 62 single SCP-like domain molecules) in *H. contortus*, 43 of which were specifically transcribed in both of these stages (Schwarz et al., 2013). The original number of predicted SCP/TAP proteins ($n = 84$) was likely inflated compared with the 21 proteins detected in the present study due to the fragmentation typical of draft genomes assembled from short DNA sequence read data (Korhonen et al., 2016). Sequences of these 21 matched those in the set of 45 predicted from transcriptomic data sets from a previous study (Mohandas et al., 2015). The discrepancy in number between this and the previous study can be explained, to some extent, by detectable proteins being present exclusively in the soma of the worm, or simply by an inability of the present quantitative proteomic approach to detect tiny amounts of proteins in a complex suspension of molecules from the parasite (Schubert et al., 2017). Further work is required to estimate the number of proteins present in ES products from all stages of *H. contortus*. By comparing the 21 detected proteins with those inferred from transcriptomic data (Mohandas et al., 2015), ~ 23 would be expected to be in ES products, provided that they are detectable using current proteomic tools (analytical sensitivity of 1×10^{-15} g) (Yates et al., 2009), but further work is required to confirm this proposal. The previous discovery of only two SCP/TAPS proteins (i.e. Hc24 – single SCP-like domain, and Hc40 – double SCP-like domain) in ES products from adult *H. contortus* (see Yatsuda et al., 2003) likely related to the limited level of sensitivity of the two-dimensional, gel-based proteomic method used and the absence of a genome at the time of investigation.

Besides SCP/TAPS proteins, proteins of the C-lectin family were abundant in different developmental stages (cf. Supplementary

Table S9). C-type lectins are carbohydrate-binding proteins (McGreal et al., 2004; Mulvenna et al., 2009) and likely play roles in parasitism, immune evasion (Harcus et al., 2009), defence against microbes (Mallo et al., 2002) and/or fertilisation (Brown et al., 2007). Molecular evidence indicates that the C-type lectin CLEC-50 has an 'inducible' antibacterial effect in the free-living nematode *C. elegans* (see Mallo et al., 2002). In parasitic nematodes, similar C-type lectin homologues have been shown to be expressed primarily in the adult stages of the strongylid nematodes *Heligmosomoides polygyrus* and *Nippostrongylus brasiliensis*, suggesting an anti-bacterial role (Harcus et al., 2009). However, at least 270 C-type lectins have been inferred for *C. elegans* (see Schulenburg et al., 2008), whereas eight C-type lectins were detected here in the proteome of *H. contortus*, with 46 predicted previously from the draft genome of this worm (Schwarz et al., 2013); this difference in number likely relates to the fragmentation that is characteristic of draft genomes (Korhonen et al., 2016).

Given that most C-type lectins are expressed in a pathogen-specific manner in *C. elegans* (i.e. one particular C-type lectin expressed to defend against one particular pathogen species) (Schulenburg et al., 2008), it is likely that the regulation of these lectins in defence against bacterial infections is distinct between *C. elegans* and *H. contortus*. One C-type lectin in *H. contortus* might respond to multiple pathogens species, although this worm (at the L4 and adult stages) lives in what could be considered a sterile environment (pH 1.0 in the abomasum). It would be interesting to establish whether C-type lectins are upregulated in this parasitic nematode in response to particular pathogens or microbes. It is also possible that some C-type lectins play a role in immune evasion, as it is known that TES-70 in *Toxocara canis* and *As*-CTL-1 in *Ascaris suum* exhibit sequence homology (28–31%) to host immune cell receptors (e.g., CD23 and macrophage mannose receptor) (Loukas et al., 1999; Yoshida et al., 2012), and they have been reported to bind mammalian carbohydrates in a calcium-dependent manner (Loukas et al., 2000). This information suggests a role for C-type lectins in immune evasion by parasitic nematodes either via inhibiting the migration of host cells or by binding to, or masking worm carbohydrates from/on host immune cells. The abundant expression of C-type lectins in parasitic stages of *H. contortus* (see Supplementary Table S9) suggests that these proteins could be involved in immune evasion or avoidance in the host animal. Interestingly, four C-type lectins, HCON_2564s, HCON_6854s, HCON_8701s and HCON_8702s, were present at high levels in the egg stage of *H. contortus* (see Supplementary Table S9). A previous study of a related strongylid, *Ancylostoma ceylanicum* (hookworm), showed that a C-type lectin, designated *Ace*-CTL-1, expressed in the sperm and testes of adult males, and the spermatheca and developing embryos within adult females, is involved in reproductive and developmental processes of this hookworm (Brown et al., 2007). This information stimulates further explorations of the functional roles of HCON_2564s, HCON_6854s, HCON_8701s and HCON_8702s in *H. contortus*.

In conclusion, here we report the somatic proteome of the barber's pole worm, one of the most important pathogens of ruminants world-wide. Using a high throughput LC–MS/MS-based approach, we confidently quantified a total of 2487 proteins in key developmental stages (i.e., egg, L3, L4 and adults) and observed marked proteomic alterations during the developmental transition from the free-living to the parasitic stages, particularly for molecules inferred to play essential roles in host invasion, development and survival (i.e. nutrition metabolism, cuticle synthesis/turnover, parasite-host communication/interaction, blood feeding and detoxification), suggesting a fine biological balance between the parasite and the host animal. The present results now complement and further enhance the value of transcriptomic and genomic data sets, will enable new insights into the biology of this highly significant parasitic nematode and should underpin work toward new anti-parasite interventions in this post-genomics era. From a technical perspective, this study indicates the major advantages of a high throughput LC–MS/MS-based approach to support systems biology explorations of parasitic nematodes and encourages proteomic studies of other socio-economically important parasitic nematodes.

Acknowledgements

Funding from the National Health and Medical Research Council (NHMRC) of Australia, the Australian Research Council, Melbourne Water Corporation, Australia, and The University of Melbourne (BIP), Australia, is gratefully acknowledged (R.B.G. et al.) as is support from the Melbourne Bioinformatics Platform, Australia. P.K.K. holds an NHMRC Early Career Researcher Fellowship (ECRF). We are grateful to Mr Qiang Huang for his support in the preparation of Fig. 2. Funding bodies played no role in the design of the study or collection, analysis or interpretation of data, or in the writing of the manuscript.

Appendix A. Supplementary data

Supplementary data to this article can be found online at https://doi.org/10.1016/j.ijpara.2018.12.003.

References

Aebersold, R., Mann, M., 2016. Mass-spectrometric exploration of proteome structure and function. Nature 537, 347–355.

Ang, C.S., Binos, S., Knight, M.I., Moate, P.J., Cocks, B.G., McDonagh, M.B., 2011. Global survey of the bovine salivary proteome: integrating multidimensional prefractionation, targeted, and glycocapture strategies. J. Proteome Res. 10, 5059–5069.

Armstrong, S.D., Xia, D., Bah, G.S., Krishna, R., Ngangyung, H.F., LaCourse, E.J., McSorley, H.J., Kengne-Ouafo, J.A., Chounna-Ndongmo, P.W., Wanji, S., Enyong, P.A., Taylor, D.W., Blaxter, M.L., Wastling, J.M., Tanya, V.N., Makepeace, B.L., 2016. Stage-specific proteomes from *Onchocerca ochengi*, sister species of the human river blindness parasite, uncover adaptations to a nodular lifestyle. Mol. Cell. Proteomics 15, 2554–2575.

Ashrafi, K., 2007. Obesity and the Regulation of Fat Metabolism. WormBook (http://www.wormbook.org/), pp. 1–20.

Bennuru, S., Meng, Z., Ribeiro, J.M., Semnani, R.T., Ghedin, E., Chan, K., Lucas, D.A., Veenstra, T.D., Nutman, T.B., 2011. Stage-specific proteomic expression patterns of the human filarial parasite *Brugia malayi* and its endosymbiont *Wolbachia*. Proc. Natl. Acad. Sci. U. S. A. 108, 9649–9654.

Brown, A.C., Harrison, L.M., Kapulkin, W., Jones, B.F., Sinha, A., Savage, A., Villalon, N., Cappello, M., 2007. Molecular cloning and characterization of a C-type lectin from *Ancylostoma ceylanicum*: evidence for a role in hookworm reproductive physiology. Mol. Biochem. Parasitol. 151, 141–147.

Bruderer, R., Bernhardt, O.M., Gandhi, T., Miladinovic, S.M., Cheng, L.Y., Messner, S., Ehrenberger, T., Zanotelli, V., Butscheid, Y., Escher, C., Vitek, O., Rinner, O., Reiter, L., 2015. Extending the limits of quantitative proteome profiling with data-independent acquisition and application to acetaminophen-treated three-dimensional liver microtissues. Mol. Cell. Proteomics 14, 1400–1410.

Bruderer, R., Bernhardt, O.M., Gandhi, T., Reiter, L., 2016. High-precision iRT prediction in the targeted analysis of data-independent acquisition and its impact on identification and quantitation. Proteomics 16, 2246–2256.

Buck, A.H., Coakley, G., Simbari, F., McSorley, H.J., Quintana, J.F., Le Bihan, T., Kumar, S., Abreu-Goodger, C., Lear, M., Harcus, Y., Ceroni, A., Babayan, S.A., Blaxter, M., Ivens, A., Maizels, R.M., 2014. Exosomes secreted by nematode parasites transfer small RNAs to mammalian cells and modulate innate immunity. Nat. Commun. 5, 5488.

Caito, S.W., Aschner, M., 2015. Quantification of glutathione in *Caenorhabditis elegans*. Curr. Protoc. Toxicol. 64, 1–6.

Campbell, B.E., Nagaraj, S.H., Hu, M., Zhong, W., Sternberg, P.W., Ong, E.K., Loukas, A., Ranganathan, S., Beveridge, I., McInnes, R.L., Hutchinson, G.W., Gasser, R.B., 2008. Gender-enriched transcripts in *Haemonchus contortus*–predicted functions and genetic interactions based on comparative analyses with *Caenorhabditis elegans*. Int. J. Parasitol. 38, 65–83.

Chehayeb, J.F., Robertson, A.P., Martin, R.J., Geary, T.G., 2014. Proteomic analysis of adult *Ascaris suum* fluid compartments and secretory products. PLoS Negl. Trop. Dis. 8, e2939.

Cooper, A.F., Van Gundy, S.D., 1971. Ethanol production and utilization by *Aphelenchus avenae* and *Caenorhabditis* sp. J. Nematol. 3, 205–214.

Gasser, R.B., von Samson-Himmelstjerna, G., 2016. *Haemonchus contortus* and haemonchosis – past, present and future trends. Adv Parasitol. Academic Press, London, UK.
Gibbs, G.M., Roelants, K., O'Bryan, M.K., 2008. The CAP superfamily: cysteine-rich secretory proteins, antigen 5, and pathogenesis-related 1 proteins–roles in reproduction, cancer, and immune defense. Endocr. Rev. 29, 865–897.
Harcus, Y., Nicoll, G., Murray, J., Filbey, K., Gomez-Escobar, N., Maizels, R.M., 2009. C-type lectins from the nematode parasites *Heligmosomoides polygyrus* and *Nippostrongylus brasiliensis*. Parasitol. Int. 58, 461–470.
Harder, A., 2016. The biochemistry of *Haemonchus contortus* and other parasitic nematodes. Adv. Parasitol. 93, 69–94.
Hewitson, J.P., Filbey, K.J., Esser-von Bieren, J., Camberis, M., Schwartz, C., Murray, J., Reynolds, L.A., Blair, N., Robertson, E., Harcus, Y., Boon, L., Huang, S.C., Yang, L., Tu, Y., Miller, M.J., Voehringer, D., Le Gros, G., Harris, N., Maizels, R.M., 2015. Concerted activity of IgG1 antibodies and IL-4/IL-25-dependent effector cells trap helminth larvae in the tissues following vaccination with defined secreted antigens, providing sterile immunity to challenge infection. PLoS Pathog. 11, e1004676.
Hewitson, J.P., Harcus, Y.M., Curwen, R.S., Dowle, A.A., Atmadja, A.K., Ashton, P.D., Wilson, A., Maizels, R.M., 2008. The secretome of the filarial parasite, *Brugia malayi*: proteomic profile of adult excretory-secretory products. Mol. Biochem. Parasitol. 160, 8–21.
Howe, K.L., Bolt, B.J., Cain, S., Chan, J., Chen, W.J., Davis, P., Done, J., Down, T., Gao, S., Grove, C., Harris, T.W., Kishore, R., Lee, R., Lomax, J., Li, Y., Muller, H.M., Nakamura, C., Nuin, P., Paulini, M., Raciti, D., Schindelman, G., Stanley, E., Tuli, M.A., Van Auken, K., Wang, D., Wang, X., Williams, G., Wright, A., Yook, K., Berriman, M., Kersey, P., Schedl, T., Stein, L., Sternberg, P.W., 2016. WormBase 2016: expanding to enable helminth genomic research. Nucleic Acids Res. 44, 774–780.
Kall, L., Canterbury, J.D., Weston, J., Noble, W.S., MacCoss, M.J., 2007. Semi-supervised learning for peptide identification from shotgun proteomics datasets. Nat. Methods 4, 923–925.
Kanehisa, M., Sato, Y., Kawashima, M., Furumichi, M., Tanabe, M., 2016. KEGG as a reference resource for gene and protein annotation. Nucleic Acids Res. 44, D457–D462.
Korhonen, P.K., Young, N.D., Gasser, R.B., 2016. Making sense of genomes of parasitic worms: tackling bioinformatic challenges. Biotechnol. Adv. 34, 663–686.
Laing, R., Kikuchi, T., Martinelli, A., Tsai, I.J., Beech, R.N., Redman, E., Holroyd, N., Bartley, D.J., Beasley, H., Britton, C., Curran, D., Devaney, E., Gilabert, A., Hunt, M., Jackson, F., Johnston, S.L., Kryukov, I., Li, K., Morrison, A.A., Reid, A.J., Sargison, N., Saunders, G.I., Wasmuth, J.D., Wolstenholme, A., Berriman, M., Gilleard, J.S., Cotton, J.A., 2013. The genome and transcriptome of *Haemonchus contortus*, a key model parasite for drug and vaccine discovery. Genome Biol. 14, R88.
Liu, R.D., Cui, J., Liu, X.L., Jiang, P., Sun, G.G., Zhang, X., Long, S.R., Wang, L., Wang, Z. Q., 2015. Comparative proteomic analysis of surface proteins of *Trichinella spiralis* muscle larvae and intestinal infective larvae. Acta Trop. 150, 79–86.
Loukas, A., Doedens, A., Hintz, M., Maizels, R.M., 2000. Identification of a new C-type lectin, TES-70, secreted by infective larvae of *Toxocara canis*, which binds to host ligands. Parasitology 121, 545–554.
Loukas, A., Mullin, N.P., Tetteh, K.K., Moens, L., Maizels, R.M., 1999. A novel C-type lectin secreted by a tissue-dwelling parasitic nematode. Curr. Biol. 9, 825–828.
Ma, G., Wang, T., Korhonen, P.K., Ang, C., Williamson, N.A., Young, N.D., Stroehlein, A.J., Hall, R.S., Koehler, A.V., Hofmann, A., Gasser, R.B., 2018. Molecular alterations during larval development of *Haemonchus contortus* in vitro are under tight post-transcriptional control. Int. J. Parasitol. 48, 763–772.
Mallo, G.V., Kurz, C.L., Couillault, C., Pujol, N., Granjeaud, S., Kohara, Y., Ewbank, J.J., 2002. Inducible antibacterial defense system in *C. elegans*. Curr. Biol. 12, 1209–1214.
Mao, X., Cai, T., Olyarchuk, J.G., Wei, L., 2005. Automated genome annotation and pathway identification using the KEGG Orthology (KO) as a controlled vocabulary. Bioinformatics 21, 3787–3793.
Martin, J., Rosa, B.A., Ozersky, P., Hallsworth-Pepin, K., Zhang, X., Bhonagiri-Palsikar, V., Tyagi, R., Wang, Q., Choi, Y.J., Gao, X., McNulty, S.N., Brindley, P.J., Mitreva, M., 2015. Helminth.net: expansions to Nematode.net and an introduction to Trematode.net. Nucleic Acids Res. 43, D698–D706.
Mes, T.H., Eysker, M., Ploeger, H.W., 2007. A simple, robust and semi-automated parasite egg isolation protocol. Nat. Protoc. 2, 486–489.
Mohandas, N., Young, N.D., Jabbar, A., Korhonen, P.K., Koehler, A.V., Amani, P., Hall, R.S., Sternberg, P.W., Jex, A.R., Hofmann, A., Gasser, R.B., 2015. The barber's pole worm CAP protein superfamily–A basis for fundamental discovery and biotechnology advances. Biotechnol. Adv. 33, 1744–1754.
Mohandas, N., Young, N.D., Jabbar, A., Korhonen, P.K., Koehler, A.V., Hall, R.S., Hu, M., Hofmann, A., Gasser, R.B., 2016. The complement of family M1 aminopeptidases of *Haemonchus contortus*–biotechnological implications. Biotechnol. Adv. 34, 65–76.
Morris, C.P., Bennuru, S., Kropp, L.E., Zweben, J.A., Meng, Z., Taylor, R.T., Chan, K., Veenstra, T.D., Nutman, T.B., Mitre, E., 2015. A proteomic analysis of the body wall, digestive tract, and reproductive tract of *Brugia malayi*. PLoS Negl. Trop. Dis. 9, e0004054.
Mitchell, A., Chang, H.Y., Daugherty, L., Fraser, M., Hunter, S., Lopez, R., McAnulla, C., McMenamin, C., Nuka, G., Pesseat, S., Sangrador-Vegas, A., Scheremetjew, M., Rato, C., Yong, S.Y., Bateman, A., Punta, M., Attwood, T.K., Sigrist, C.J., Redaschi, N., Rivoire, C., Xenarios, I., Kahn, D., Guyot, D., Bork, P., Letunic, I., Gough, J., Oates, M., Haft, D., Huang, H., Natale, D.A., Wu, C.H., Orengo, C., Sillitoe, I., Mi, H., Thomas, Finn, R.D., . The InterPro protein families database: the classification resource after 15 years. Nucleic Acids Res. 43, D213–D221.
McGreal, E.P., Martinez-Pomares, L., Gordon, S., 2004. Divergent roles for C-type lectins expressed by cells of the innate immune system. Mol. Immunol. 41, 1109–1121.
Mulvenna, J., Hamilton, B., Nagaraj, S.H., Smyth, D., Loukas, A., Gorman, J.J., 2009. Proteomics analysis of the excretory/secretory component of the blood-feeding stage of the hookworm *Ancylostoma caninum*. Mol. Cell. Proteomics 8, 109–121.
Nikolaou, S., Hartman, D., Presidente, P.J., Newton, S.E., Gasser, R.B., 2002. HcSTK, a *Caenorhabditis elegans* PAR-1 homologue from the parasitic nematode, *Haemonchus contortus*. Int. J. Parasitol. 32, 749–758.
Page, A.P., Johnstone, I.L. 2007. The Cuticle. WormBook (http://www.wormbook.org/), pp. 1–15.
Parkinson, J., Whitton, C., Schmid, R., Thomson, M., Blaxter, M., 2004. NEMBASE: a resource for parasitic nematode ESTs. Nucleic Acids Res. 32, D427–D430.
Preston, S., Korhonen, P.K., Mouchiroud, L., Cornaglia, M., McGee, S.L., Young, N.D., Davis, R.A., Crawford, S., Nowell, C., Ansell, B.R.E., Fisher, G.M., Andrews, K.T., Chang, B.C.H., Gijs, M.A.M., Sternberg, P.W., Auwerx, J., Baell, J., Hofmann, A., Jabbar, A., Gasser, R.B., 2017. Deguelin exerts potent nematocidal activity via the mitochondrial respiratory chain. FASEB J. 31, 4515–4532.
Roeber, F., Jex, A.R., Gasser, R.B., 2013. Next-generation molecular-diagnostic tools for gastrointestinal nematodes of livestock, with an emphasis on small ruminants: a turning point? Adv. Parasitol. 83, 267–333.
Schubert, O.T., Rost, H.L., Collins, B.C., Rosenberger, G., Aebersold, R., 2017. Quantitative proteomics: challenges and opportunities in basic and applied research. Nat. Protoc. 12, 1289–1294.
Schulenburg, H., Hoeppner, M.P., Weiner 3rd, J., Bornberg-Bauer, E., 2008. Specificity of the innate immune system and diversity of C-type lectin domain (CTLD) proteins in the nematode *Caenorhabditis elegans*. Immunobiology 213, 237–250.
Schwarz, E.M., Hu, Y., Antoshechkin, I., Miller, M.M., Sternberg, P.W., Aroian, R.V., 2015. The genome and transcriptome of the zoonotic hookworm *Ancylostoma ceylanicum* identify infection-specific gene families. Nat. Genet. 47, 416–422.
Schwarz, E.M., Korhonen, P.K., Campbell, B.E., Young, N.D., Jex, A.R., Jabbar, A., Hall, R.S., Mondal, A., Howe, A.C., Pell, J., Hofmann, A., Boag, P.R., Zhu, X.Q., Gregory, T., Loukas, A., Williams, B.A., Antoshechkin, I., Brown, C., Sternberg, P.W., Gasser, R.B., 2013. The genome and developmental transcriptome of the strongylid nematode *Haemonchus contortus*. Genome Biol. 14, R89.
Sperotto, R.L., Kremer, F.S., Aires Berne, M.E., Costa de Avila, L.F., da Silva Pinto, L., Monteiro, K.M., Caumo, K.S., Ferreira, H.B., Berne, N., Borsuk, S., 2017. Proteomic analysis of *Toxocara canis* excretory and secretory (TES) proteins. Mol. Biochem. Parasitol. 211, 39–47.
Stoltzfus, J.D., Pilgrim, A.A., Herbert, D.R., 2017. Perusal of parasitic nematode 'omics in the post-genomic era. Mol. Biochem. Parasitol. 215, 11–22.
Stroehlein, A.J., Young, N.D., Korhonen, P.K., Jabbar, A., Hofmann, A., Sternberg, P.W., Gasser, R.B., 2015. The *Haemonchus contortus* kinome–a resource for fundamental molecular investigations and drug discovery. Parasit. Vectors 8, 623.
Tang, Y.T., Gao, X., Rosa, B.A., Abubucker, S., Hallsworth-Pepin, K., Martin, J., Tyagi, R., Heizer, E., Zhang, X., Bhonagiri-Palsikar, V., Minx, P., Warren, W.C., Wang, Q., Zhan, B., Hotez, P.J., Sternberg, P.W., Dougall, A., Gaze, S.T., Mulvenna, J., Sotillo, J., Ranganathan, S., Rabelo, E.M., Wilson, R.K., Felgner, P.L., Bethony, J., Hawdon, J.M., Gasser, R.B., Loukas, A., Mitreva, M., 2014. Genome of the human hookworm *Necator americanus*. Nat. Genet. 46, 261–269.
Tort, J., Brindley, P.J., Knox, D., Wolfe, K.H., Dalton, J.P., 1999. Proteinases and associated genes of parasitic helminths. Adv. Parasitol. 43, 161–266.
Tyagi, R., Joachim, A., Ruttkowski, B., Rosa, B.A., Martin, J.C., Hallsworth-Pepin, K., Zhang, X., Ozersky, P., Wilson, R.K., Ranganathan, S., Sternberg, P.W., Gasser, R. B., Mitreva, M., 2015. Cracking the nodule worm code advances knowledge of parasite biology and biotechnology to tackle major diseases of livestock. Biotechnol. Adv. 33, 980–991.
Tyanova, S., Temu, T., Sinitcyn, P., Carlson, A., Hein, M.Y., Geiger, T., Mann, M., Cox, J., 2016. The Perseus computational platform for comprehensive analysis of (prote)omics data. Nat. Methods 13, 731–740.
Tzelos, T., Matthews, J.B., Buck, A.H., Simbari, F., Frew, D., Inglis, N.F., McLean, K., Nisbet, A.J., Whitelaw, C.B., Knox, D.P., McNeilly, T.N., 2016. A preliminary proteomic characterisation of extracellular vesicles released by the ovine parasitic nematode, *Teladorsagia circumcincta*. Vet. Parasitol. 221, 84–92.
Uchiyama, T., Irie, M., Mori, H., Kurokawa, K., Yamada, T., 2015. FuncTree: functional analysis and visualization for large-scale omics data. PLoS One 10, e0126967.
Veglia, F., 1915. The anatomy and life-history of the *Haemonchus contortus* (Rud.). Rep. Dir. Vet. Res. 3–4, 347–500.
Wang, T., Nie, S., Ma, G., Korhonen, P.K., Koehler, A.V., Ang, C., Reid, G.E., Williamson, N.A., Gasser, R.B., 2018. The developmental lipidome of *Haemonchus contortus*. Int. J. Parasitol. 48, 887–895.
Wang, T., Van Steendam, K., Dhaenens, M., Vlaminck, J., Deforce, D., Jex, A.R., Gasser, R.B., Geldhof, P., 2013. Proteomic analysis of the excretory-secretory products from larval stages of *Ascaris suum* reveals high abundance of glycosyl hydrolases. PLoS Negl. Trop. Dis. 7, e2467.
Williamson, A.L., Brindley, P.J., Knox, D.P., Hotez, P.J., Loukas, A., 2003. Digestive proteases of blood-feeding nematodes. Trends Parasitol. 19, 417–423.
Xie, C., Mao, X., Huang, J., Ding, Y., Wu, J., Dong, S., Kong, L., Gao, G., Li, C.Y., Wei, L., 2011. KOBAS 2.0: a web server for annotation and identification of enriched pathways and diseases. Nucleic Acids Res. 39, W316–W322.
Yates, J.R., Ruse, C.I., Nakorchevsky, A., 2009. Proteomics by mass spectrometry: approaches, advances, and applications. Annu. Rev. Biomed. Eng. 11, 49–79.

Yatsuda, A.P., Krijgsveld, J., Cornelissen, A.W., Heck, A.J., de Vries, E., 2003. Comprehensive analysis of the secreted proteins of the parasite *Haemonchus contortus* reveals extensive sequence variation and differential immune recognition. J. Biol. Chem. 278, 16941–16951.

Yoshida, A., Nagayasu, E., Horii, Y., Maruyama, H., 2012. A novel C-type lectin identified by EST analysis in tissue migratory larvae of *Ascaris suum*. Parasitol Res. 110, 1583–1586.

Zamanian, M., Fraser, L.M., Agbedanu, P.N., Harischandra, H., Moorhead, A.R., Day, T. A., Bartholomay, L.C., Kimber, M.J., 2015. Release of small RNA-containing exosome-like vesicles from the human filarial parasite *Brugia malayi*. PLoS Negl. Trop. Dis. 9, e0004069.

Zhang, Y., Fonslow, B.R., Shan, B., Baek, M.C., Yates 3rd., J.R., 2013. Protein analysis by shotgun/bottom-up proteomics. Chem. Rev. 113, 2343–2394.